Article

Tetraborylation of *p*-Benzynes Generated by the Masamune−Bergman Cyclization through Reaction Design Based on the Reaction Path Network

Soichiro Nakatsuka, Seiji Akiyama, Yu Harabuchi, Satoshi Maeda, and Yuuya Nagata*

Read Online

ACCESS | Metrics & More | Article Recommendations | SI Supporting Information

ABSTRACT: Designing the reactant molecule of an initial reaction, based on quantum chemical pathway exploration, enabled us to access a new reaction, i.e., the tetraborylation reaction of *p*-benzynes generated from 1,2-diethynylbenzene derivatives, using bis(pinacolato)diborane(4) (B_2pin_2). Based on the reaction path network generated via the artificial-force-induced reaction (AFIR) method, desired and undesired paths were identified and used to modify the chemical structure of the reactant. After the in silico screening, the optimal structure of the reactant was determined to be a 1,2-diethynylbenzene derivative with a butylene linker. The reaction of the optimized reactant and its derivatives with an excess of B_2pin_2 gave the tetraborylated products in good yields (up to 58%). It is quite intriguing that the two carbons of *p*-benzyne behave formally as dicarbenes in this reaction.

Design of Chemical Reaction Using Reaction Path Network

Modification of the Reaction by *In Silico* Analysis

(excess)

140 °C, 16 h

New Tetraborylation Reaction

KEYWORDS: *quantum chemical calculation, reaction path, reaction path network, reaction discovery, borylation reaction*
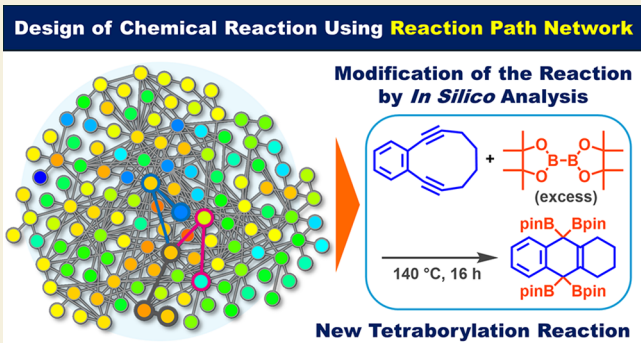
INTRODUCTION

Organoboron compounds are an essential class of versatile building blocks for functional materials and pharmaceutical compounds.[1−4] Arylboronic acids and their analogous esters are widely used because of their versatility in conversion to various functional groups.[5−7] Based on the high demand for these organoboron compounds, synthetic methods to access them are well developed.[8−12] On the other hand, although various techniques to prepare organoboron compounds have been developed, reports of reactions involving multiple borylation at the same carbon atom are still limited despite high interest in them.[13−17] To develop new multiborylation reactions, we focused our attention on *p*-benzynes generated by the Masamune−Bergman cyclization[18−23] of enediynes because of their high reactivity.

In recent years, theoretical chemistry has been essential in revealing the structures of molecules and their physical properties. In organic chemistry, quantum chemical calculations are crucial for obtaining mechanistic insight into chemical reactions. We have developed the artificial-force-induced reaction (AFIR) method,[24] one of the automated reaction path search methods.[25] The AFIR method induces structural changes by applying a virtual artificial force between molecules or fragments within a molecule or a complex. Even when only the product is known, AFIR can predict reactions by tracing back the network of its formation paths from the product side, guided by inverse kinetic analysis.[26] To date,

various reactions suggested using the AFIR method have been experimentally demonstrated.[27−30] However, in previous studies, modifications of the chemical structures of the reactants based on experiments were still necessary to enable the expected reactions. Here, we focused on a systematic strategy based on a reaction path network to modify the reactants in an initial reaction to develop a new reaction affording the desired product (Figure 1). For example, in the initial reaction, the starting material (**SM**) might give undesired product **Prod. A** through intermediate **Int**. Guided by in silico analysis, **SM** would be modified to **SM-mod**, affording desired product **Prod. B** through intermediate **Int-mod** and leading to the discovery of a new reaction.

In this study, we first investigated the borylation reaction of *p*-benzynes generated by the Masamune−Bergman cyclization reaction by using the AFIR method. Subsequently, we accessed the map of the reaction paths to determine how to modify the substrate structure to obtain the target compound using theoretical calculations. Finally, we experimentally investigated
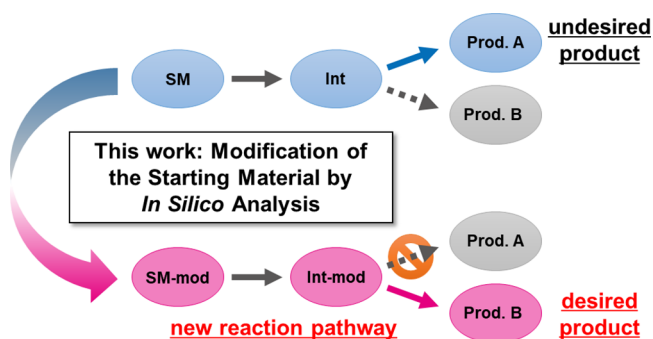
Figure 1. Our concept of theoretical-calculation-based modification of the initial reactant to develop a new reaction affords the desired product. **SM:** starting material, **SM-mod:** modified starting material, **Int.:** intermediate, **Int-mod:** modified intermediate, and **Prod. A** and **B**: Products.

the tetraborylation reaction of 1,2-diethynylbenzene derivatives and bis(pinacolato)diborane(4) (B₂pin₂).

RESULTS AND DISCUSSION

First, we started preliminary calculations using the AFIR method with the Global Reaction Route Mapping (GRRM) program.[31] To investigate the reaction conditions for the reaction of an enediyne with diborane(4) compounds, we carried out an automated reaction path search method, namely,

the single component artificial force induced reaction (SC-AFIR) method with density-functional theory (DFT) calculations at the UB3LYP/6-31G level of theory. Here, the SC-AFIR performs automated generation of global or semiglobal reaction path networks, which consist of equilibrium (EQ) structures and transition states (TS) of chemical reactions.[32,33] In this study, the kinetic navigation option was used to navigate the SC-AFIR search based on kinetic simulation.[34] The kinetic SC-AFIR search, also called forward on-the-fly kinetic simulation,[35] generates a reaction path network that exhaustively includes paths within the kinetically accessible region on the potential energy surface and those that cross the boundary between kinetically accessible and inaccessible regions. In the preliminary calculations, (Z)-hex-3-en-1,5-diyne (**1a**) and bis(ethylene glycolato)diborane(4) (B₂eg₂) were employed as an enediyne and a diborane(4) compound to reduce the computational load. A reaction path network was calculated for the reaction of the enediyne with 1 equiv of B₂eg₂ (Figure 2a,b). The Masamune−Bergman cyclization from the enediyne to *p*-benzyne gives *p*-benzyne (**A−B**) in high selectivity, with a relatively high Gibbs activation energy ($\Delta G^{\ddagger}$) of 131.6 kJ/mol. Subsequently, the generated *p*-benzyne will react with B₂eg₂ with a low $\Delta G^{\ddagger}$ (8.7 kJ/mol, **B−C**), indicating that the *p*-benzyne reacts easily with B₂eg₂. After the addition process, a branched pathway was observed. One pathway affords a diborylated product via cleavage of a B−B bond (**C−D−E**); this is the preferred pathway based on
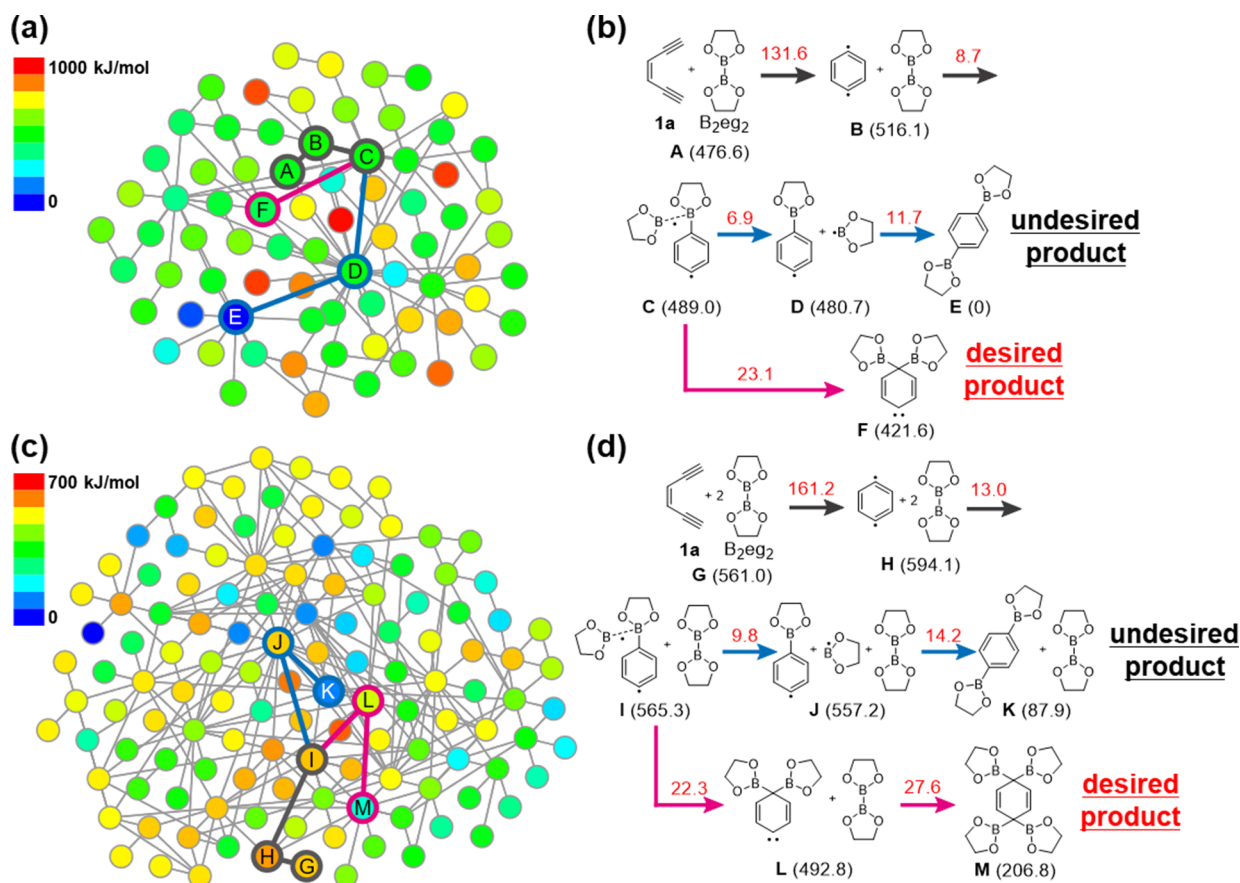

Figure 2. Reaction path network and the lowest energy pathways for the reaction of enediyne 1a with 1 equiv (a,b) or 2 equiv (c,d) of B2eg2 at the UB3LYP/6-31G level of theory. Nodes (circles) and edges (lines) represent obtained equilibrium structures and reaction paths connecting them, respectively. In (a,c), the color of the nodes represents their Gibbs energy at 300 K. In (b,d), the bracketed numbers indicate the Gibbs energy of each species, and the red numbers indicate activation energy in kJ/mol at 300 K.

the energies $\Delta G^{\ddagger}$ of each step. The other pathway affords 1,2-migration of the boryl group (**C**−**F**) and had a relatively higher $\Delta G^{\ddagger}$ than the first one (**C**−**D**−**E**).

Detailed calculations revealed that intermediate **C** is an open-shell singlet biradical that combines the features of an aryl radical and a one-electron B−B σ bond (see SI, Figure S1). This indicates that the weak one-electron B−B σ bond can be readily cleaved to induce the 1,2-boryl shift, affording intermediate **F**. According to the previous report on the 1,1-diborylation reaction of carbene with diborane(4),[14] the presence of one more equivalent of B_2eg_2 may allow further 1,1-diborylation to proceed to the carbene carbon of the intermediate **F**.

Second, we calculated a reaction path network for the reaction of the enediyne with 2 equiv of B_2eg_2 (Figure 2c,d). When an additional B_2eg_2 molecule was introduced, it was suggested that a pathway that involves an unusual tetraborylated product **M**. In order to obtain this tetraborylated product, two issues must be resolved: (1) The activation energy of the initial Masamune−Bergman cyclization must be decreased. (2) The pathway must be switched from that giving the diborylated product (**I**−**J**) to one affording the tetraborylation product (**I**−**L**).

To solve these issues and obtain the tetraborylated compound, we attempted to modify the molecular structure of the enediyne based on theoretical calculations. Here, activation energies that are too high are undesirable because the reaction does not proceed, but activation energies that are too low are also undesirable because spontaneous degradation occurs. Although the effect of the structures of the enediynes on the activation energies of the Masamune−Bergman cyclization has been studied in previous papers,[36−38] the activation energies were systematically calculated here in order to choose the substrate suitable for the experiment. First, **1a** was modified to give enediynes **2a**−**8a**, and the resulting activation energies of the Masamune−Bergman cyclization were investigated (Figure 3). **2a** having a (Z)-2-butene moiety
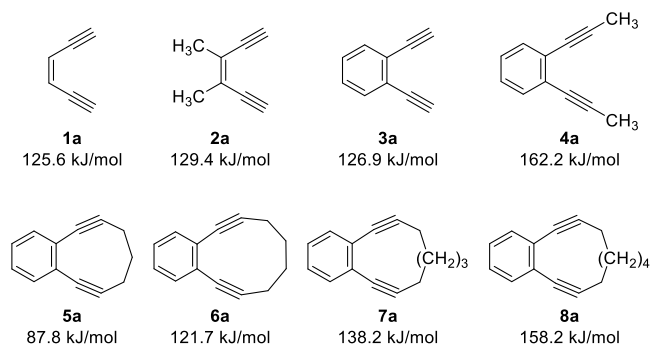
**Figure 3.** In silico analysis of the activation energies of the Masamune−Bergman cyclization of enediynes **1a**−**8a** at the UB3LYP-D3BJ/6-31G(d,p) level of theory at 298.15 K.

and **3a** having a benzene ring showed comparable activation energies to **1a**. Two prop-1-yn-1-yl groups were introduced to **4a** to suppress the degradation due to the high reactivity of the terminal alkyne structures; however, the activation energy increased to 162.2 kJ/mol, which means that this cyclization reaction will require more than 40 h at 200 °C to proceed 50%. Second, we were interested in shortening the distance between the ethynyl groups using a linker moiety based on previous reports. Linker moieties of various lengths connecting the two

ethynyl groups were introduced to **3a**, affording **5a**−**8a**. **5a** with a propylene linker showed a low activation energy (87.8 kJ/mol), which means that **5a** should be unstable at room temperature. **6a** with a butylene linker showed an appropriate activation energy for the reaction, suggesting that it could be a promising substrate. **7a** and **8a** with longer linker moieties showed higher activation energies than **6a**, suggesting that these substrates are unsuitable for this reaction.

Based on the previous screening of the activation energies of the Masamune−Bergman cyclization, **1a**−**3a** and **6a** were adopted as substrate candidates. Subsequently, we calculated the activation energies of the pathways to afford the diborylated products (**I**−**J**) or the tetraborylated products (**I**−**L**) of p-benzynes **1a′**−**3a′** and **6a′** derived from **1a**−**3a** and **6a** (Table 1). For **1a′** and **2a′**, **TS$_{I-J}$**, which gives the
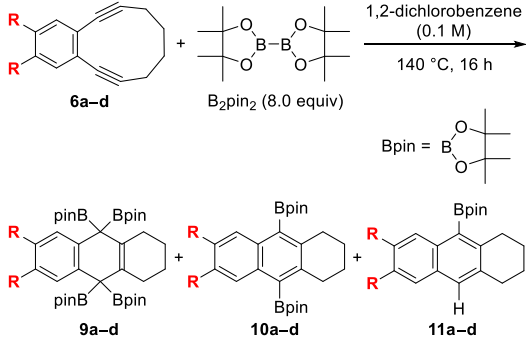
Table 1. In Silico Analysis of the Activation Energies of the Pathways To Afford the Diborylated Product (I−J) or the Tetraborylated Product (I−L) of p-Benzynes 1a′−3a′ and 6a′ at the UB3LYP-D3BJ/6-31G(d,p) Level of Theory at 298.15 K
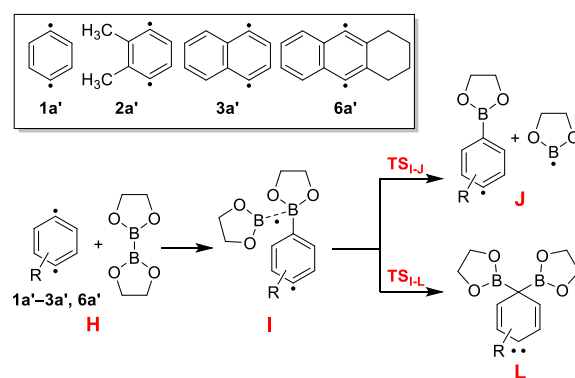
p-benzene	TS$_{I-J}$ ($\Delta G^{\ddagger}$ of I−J to afford diborylated product, kJ/mol)	TS$_{I-L}$ ($\Delta G^{\ddagger}$ of I−L to afford tetraborylated product, kJ/mol)
1a′	6.5	11.3
2a′	6.7	9.9
3a′	9.2	4.3
6a′	9.3	4.7

diborylated product, showed a lower activation energy than that of **TS$_{I-L}$**, which gives the tetraborylated product. The **TS$_{I-J}$** of **3a′** was found to be lower in energy than that of **TS$_{I-L}$**, suggesting that **3a′** would afford the tetraborylated product. **6a′** showed the highest **TS$_{I-J}$** and the lowest **TS$_{I-L}$** among these compounds, indicating that **6a′** exhibited the highest preference for the tetraborylated product. The reason for the large difference in the selectivity of **3a′** and **6a′** relative to **1a′** and **2a′** would seem to be that the unpaired electrons of **3a′** and **6a′** are located on the naphthalene ring, which has a lower aromaticity compared to the benzene ring, stabilizing the transition state **TS$_{I-L}$** toward **L**, which has collapsed aromaticity.

First, **6a** and an excess of B_2pin_2 (8 equiv) were dissolved in 1,2-dichlorobenzene and stirred at 140 °C for 16 h. The tetraborylated product **9a** was obtained as the major product (57% yield, Table 2). The diborylated product **10a** and a monoborylated product **11a** were also observed as minor products with 7.4 and 7.2% yield, respectively. Subsequently, **6b**, which is a difluorinated analog of **6a**, was examined under the same reaction conditions. The yield of tetraborylated

Table 2. Results of the Reactions of 6a−d and B₂pin₂

Bpin =

		yield (%)[b]		
substrate[a]	R	9	10	11
6a	H	57	7.4	7.2
6b	F	58	7.7	6.0
6c	MeO	32	2.7	5.8
6d	Me	35	4.3	5.8

[a]All reactions were carried out on a 0.1 mmol scale (0.1 M), and the substrates 6a−d were not recovered. [b]The yield was determined from ¹H NMR analysis using 1,1,2,2-tetrachloroethane as an internal standard.

product 9b was comparable (58%). On the other hand, 6c (a dimethyl-substituted derivative) and 6d (a dimethoxy-substituted derivative) showed lower yields of the tetraborylated products 9c (32% yield) and 9d (35% yield) compared to 6a and 6b. At this stage, we assumed that this difference was caused by the presence of C−H bonds with low bond dissociation energy in methyl or methoxy groups, i.e., the competition of hydrogen atom abstraction from p-benzyne.

A crystal structure of 9c is shown in Figure 4. The four C−B bonds of 9c (1.576 and 1.590 Å) seemed to be single bonds.
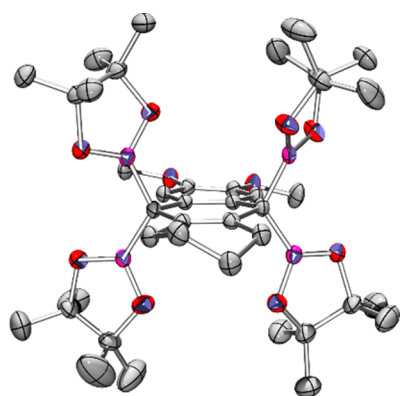

Figure 4. ORTEP drawing of 9c obtained from an X-ray crystallographic analysis. One of two independent molecules is shown. Thermal ellipsoids are shown at 50% probability, and hydrogen atoms are omitted for clarity.

The bond angles of the B−C−B bonds of 9c (114.27(16), 119.52(16), 116.43(16), and 119.14(16)) were found to be larger than ideal sp³ carbon angles, which may be caused by the steric repulsion between the bulky Bpin moieties.

To gain detailed insight into this tetraborylation reaction, we performed DFT calculations at the (U)B3LYP-D3BJ/6-311+G(2d,p)//(U)B3LYP-D3BJ/6-31G(d,p) level of theory with the solvent effect (SMD = 1,2-dichlorobenzene) for the

pathways of the reaction of 6a with B₂pin₂ to give 9a (Figure 5). The initial Masamune−Bergman cyclization from 9a to p-
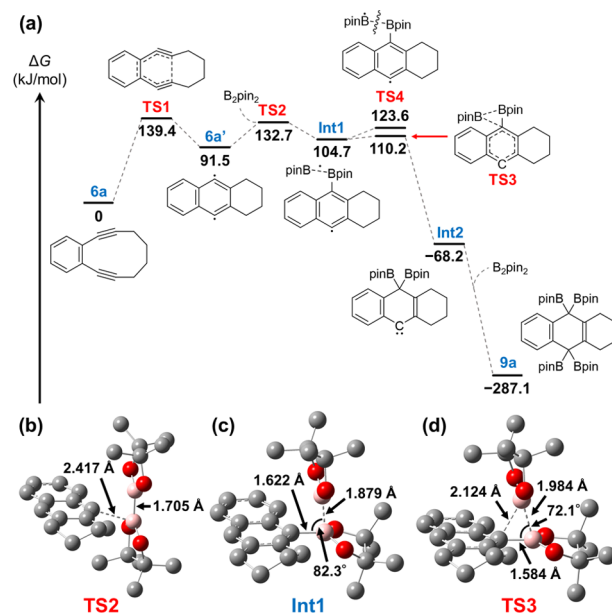

Figure 5. (a) Reaction diagram for the tetraborylation reaction of 6a with B₂pin₂ calculated at the (U)B3LYP-D3BJ/6-311+G(2d,p)//(U)B3LYP-D3BJ/6-31G(d,p) level of theory with the solvent effect (SMD = 1,2-dichlorobenzene) at 413.15 K. (b−d) Structures of TS2, Int1, and TS3 with distances and angles.

benzyne is highly selective to form the desired p-benzyne intermediate 6a via TS1 (+139.4 kJ/mol). Subsequently, the addition of B₂pin₂ to 6a occurs through TS2 with an activation energy of +41.2 kJ/mol to afford Int1. The B−B bond length in TS2 (1.705 Å) was almost the same as that of B₂pin₂ (1.701 Å) before the reaction, while in Int1 the B−B bond length was extended (1.879 Å), and a new weak B−C bond (1.622 Å) was generated (Figures 5a,b, and S2). The elongation of the B−B bond (1.879 Å) suggests that Int1 is a biradical consisting of a vinyl radical and a semioccupied B−B σ bond, the same as intermediate C (see SI, Figure S1). Next, the 1,2-migration of the boryl group in the addition intermediate occurs with an activation energy of +5.5 kJ/mol. Here, two transition states (TS3 and TS4) were found, which afford the tetraborylated and diborylated products, respectively. Importantly, the activation energy via TS3 (+5.5 kJ/mol) is lower than that via TS4 (+18.9 kJ/mol), indicating that generation of the tetraborylated product will be preferred. In TS3, the B−B distance is elongated to 1.984 Å and weakened, and the first B−C bond is further shortened to 1.584 Å and strengthened (Figure 5c). On the other hand, the distance between the other boron atom and the carbon center approaches 2.124 Å, leading to the formation of Int2 via a three-membered ring transition state consisting of B−B−C. Note that the Masamune−Bergmann cyclization is known to be a reversible reaction,[39,40] however, comparing TS1 and TS2, the energy of TS1 is 6.7 kJ/mol higher than that of TS. In addition, it can be assumed that 6a' and B₂pin₂ will react promptly under the actual reaction conditions due to the presence of the excess amount of B₂pin₂. Considering the Boltzmann distribution at the reaction temperature (413.15 K), 88% of 6a' will proceed to the reaction to generate the product 9a, and 12% may undergo the reverse reaction and return to the starting material 6a. Since

the **6a** produced by the reverse reaction process reacts again as the starting material, it is not considered to affect the yield, but it may slow down the overall rate of the reaction. As shown in Figure 3, it is noted that the introduction of a linker at the alkyne moiety decreases the activation energy of the Masamune−Bergman reaction but does not contribute significantly to the activation energy of the reverse reaction. For example, the activation energies for the reverse reaction of **6a** with a butylene linker and **4a** with methyl groups at the alkyne terminus were found to be almost identical (see SI, Figure S3).

Here, various functionalizations have been reported starting from *p*-benzyne resulting from the Masamune−Bergmann cyclization,[39,40] including zwitterionic reactions[41] and metal-catalyzed reactions.[42] While *p*-benzyne reactions generally involve ionic intermediates to give 1,4-functionalized products, this reaction is significantly different in that the 1,1-diborylation of *p*-benzyne is followed by 1,1,4,4-tetraborylation through neutral radical intermediates (Figures 5a and S1). This result suggests that our modification of the substrate based on the in silico analyses successfully prevented the undesired pathway to achieve the desired product and could be expected as a new reaction development method.

CONCLUSIONS

In summary, we have demonstrated that modifying the reactant of an initial reaction based on a reaction path network enabled us to develop a new reaction, namely, the tetraborylation reaction of 1,2-diethynylbenzene derivatives with bis(pinacolato)diborane(4). By use of the reaction path network generated via the AFIR method, the desired and undesired paths could be revealed, providing guidance for the modification of the chemical structure of the reactant. The optimal structure of the reactant was determined to be a 1,2-diethynylbenzene derivative with a butylene linker based on the additional in silico screening. The reaction of the optimized reactant with an excess of bis(pinacolato)diborane(4) gave the desired tetraborylated products in a good yield (up to 58% yield). It is intriguing that the two carbons of *p*-benzyne behave formally as a dicarbene in this reaction. Further investigations of the obtained tetraborylated products as starting materials for new chemical transformations are currently under investigation in our laboratory along with studies on the development of new reactions using the reaction path network with the additional in silico screening presented in this paper.

METHODS

Theoretical Calculation for the Reaction Path Network

The automated reaction path search was applied to two systems separately, i.e., the system including a *p*-benzyne and one bis(ethylene glycolato)diborane(4) (B_2eg_2), and the system including a *p*-benzyne and two B_2eg_2. The searches were done by the single component-artificial force induced reaction (SC-AFIR) method[24] using the GRRM program[25] interfaced with the Gaussian 16 program.[43] The electronic structure calculations were carried out in a vacuum using the unrestricted B3LYP functional (UB3LYP) with the basis function 6-31G using the Grid = FineGrid option implemented in the Gaussian 16 program. The model collision energy parameter, γ, was set to 100.0 kJ/mol. The obtained AFIR paths tend to pass through near-TSs of the corresponding reaction paths (AFIR paths), and further optimization of the AFIR path by the locally updated planes (LUP) method gives a reaction path (denoted by LUP path).[44] During the SC-AFIR searches, the EQ to which the next SC-AFIR procedure was

applied was chosen by a kinetic-based navigation method based on the rate constant matrix contraction (RCMC) method.[34] In the kinetics-based navigation, the initial population 1.0 was assigned to eq 0, and conditions of the kinetic simulations were set at 10^{-6} s and 300 K. Kinetic analyses were performed based on the Gibbs energies of the LUP path network. Gibbs energy was estimated by harmonic vibrational analysis, whereby all harmonic frequencies smaller than 50 cm^{-1} were set to 50 cm^{-1}.

General Procedures for the Tetraborylation Reaction

Procedure A (Determination of the NMR Yields). A mixture of 0.1 mmol of an enediyne and 0.8 mmol of B_2pin_2 (0.203 g) in 1,2-dichlorobenzene (1.0 mL) was heated at 140 °C in a sealed tube under a nitrogen atmosphere. After 16 h, the solvent and the residual B_2pin_2 were removed under reduced pressure (<10 Pa) at 50 and 80 °C, respectively, and then purified by silica gel chromatography or a solution of 1,1,2,2-tetrachloroethane in CDCl$_3$ was added as an internal standard and the yield was determined by ^{1}H NMR spectroscopy.

Procedure B (Isolation of the Products). A mixture of 0.5 mmol of an enediyne and 4.0 mmol of B_2pin_2 (1.02 g) in 1,2-dichlorobenzene (5.0 mL) was heated at 140 °C in a sealed tube under a nitrogen atmosphere. After 16 h, the solvent and the residual B_2pin_2 were removed under reduced pressure (<10 Pa) at 50 and 80 °C, respectively, and the crude product was purified by sublimation under reduced pressure (<5.0 × 10^{-3} Pa) or gel permeation chromatography (GPC).

ASSOCIATED CONTENT

Ⓢ Supporting Information

The Supporting Information is available free of charge at https://pubs.acs.org/doi/10.1021/jacsau.4c00302.

> Data that support the findings of this study (PDF)
> XYZ files of the calculated structures with their Gibbs energies in Figures 2, 3, and 5, and Tables 1 and 2 (ZIP)
> Crystallographic data for compounds **9c** and **10c** and the Cambridge Crystallographic Data Center reference numbers CCDC 2100639 and CCDC 2100638, respectively (ZIP)

AUTHOR INFORMATION

Corresponding Author

Yuuya Nagata − *ERATO Maeda Artificial Intelligence in Chemical Reaction Design and Discovery Project, JST, Sapporo 060-0810 Hokkaido, Japan; Institute for Chemical Reaction Design and Discovery (WPI-ICReDD), Hokkaido University, Sapporo 001-0021 Hokkaido, Japan;* ⓘ orcid.org/0000-0001-5926-5845; Email: nagata@icredd.hokudai.ac.jp

Authors

Soichiro Nakatsuka − *ERATO Maeda Artificial Intelligence in Chemical Reaction Design and Discovery Project, JST, Sapporo 060-0810 Hokkaido, Japan; Department of Chemistry, Faculty of Science, Hokkaido University, Sapporo 060-0810 Hokkaido, Japan;* ⓘ orcid.org/0000-0003-1720-8169

Seiji Akiyama − *ERATO Maeda Artificial Intelligence in Chemical Reaction Design and Discovery Project, JST, Sapporo 060-0810 Hokkaido, Japan; Institute for Chemical Reaction Design and Discovery (WPI-ICReDD), Hokkaido University, Sapporo 001-0021 Hokkaido, Japan;* ⓘ orcid.org/0000-0002-7715-4206

Yu Harabuchi − *ERATO Maeda Artificial Intelligence in Chemical Reaction Design and Discovery Project, JST,*

Sapporo 060-0810 Hokkaido, Japan; Institute for Chemical Reaction Design and Discovery (WPI-ICReDD), Hokkaido University, Sapporo 001-0021 Hokkaido, Japan; ⓞ orcid.org/0000-0001-8313-3236

Satoshi Maeda − *ERATO Maeda Artificial Intelligence in Chemical Reaction Design and Discovery Project, JST, Sapporo 060-0810 Hokkaido, Japan; Department of Chemistry, Faculty of Science, Hokkaido University, Sapporo 060-0810 Hokkaido, Japan; Institute for Chemical Reaction Design and Discovery (WPI-ICReDD), Hokkaido University, Sapporo 001-0021 Hokkaido, Japan; Research and Services Division of Materials Data and Integrated System (MaDIS), National Institute for Materials Science (NIMS), Tsukuba 305-0044 Ibaraki, Japan;* ⓞ orcid.org/0000-0001-8822-1147

Complete contact information is available at:
https://pubs.acs.org/10.1021/jacsau.4c00302

Author Contributions

CRediT: **Soichiro Nakatsuka** conceptualization, data curation, funding acquisition, investigation, methodology, visualization, writing-original draft; **Seiji Akiyama** data curation, investigation, methodology, validation, visualization; **Yu Harabuchi** data curation, investigation, methodology, software, validation, visualization; **Satoshi Maeda** conceptualization, formal analysis, funding acquisition, project administration, software, supervision; **Yuuya Nagata** conceptualization, data curation, funding acquisition, project administration, supervision, validation, visualization, writing-review & editing.

Notes

The authors declare no competing financial interest.

■ REFERENCES

(1) Yan, J.; Fang, H.; Wang, B. Boronolectins and fluorescent boronolectins: An examination of the detailed chemistry issues important for the design. *Med. Res. Rev.* **2005**, *25*, 490−520.

(2) Trippier, P. C.; McGuigan, C. Boronic acids in medicinal chemistry: Anticancer, antibacterial and antiviral applications. *MedChemComm* **2010**, *1*, 183−198.

(3) Smoum, R.; Rubinstein, A.; Dembitsky, V. M.; Srebnik, M. Boron containing compounds as protease inhibitors. *Chem. Rev.* **2012**, *112*, 4156−4220.

(4) Brooks, W. L. A.; Sumerlin, B. S. Synthesis and Applications of Boronic Acid-Containing Polymers: From Materials to Medicine. *Chem. Rev.* **2016**, *116*, 1375−1397.

(5) Kabalka, G. W. Boron: Boranes in organic synthesis. *J. Organomet. Chem.* **1984**, *274*, 1−29.

(6) Miyaura, N.; Suzuki, A. Palladium-Catalyzed Cross-Coupling Reactions of Organoboron Compounds. *Chem. Rev.* **1995**, *95*, 2457−2483.

(7) Pattison, G. Fluorination of organoboron compounds. *Org. Biomol. Chem.* **2019**, *17*, 5651−5660.

(8) Brown, H. C. Organoboranes - The Modern Miracle. *Pure Appl. Chem.* **1976**, *47*, 49−60.

(9) Mkhalid, I. A. I.; Barnard, J. H.; Marder, T. B.; Murphy, J. M.; Hartwig, J. F. C-H activation for the construction of C-B bonds. *Chem. Rev.* **2010**, *110*, 890−931.

(10) Wang, M.; Shi, Z. Methodologies and Strategies for Selective Borylation of C-Het and C-C Bonds. *Chem. Rev.* **2020**, *120*, 7348−7398.

(11) Bose, S. K.; Deissenberger, A.; Eichhorn, A.; Steel, P. G.; Lin, Z. Y.; Marder, T. B. Zinc-Catalyzed Dual C-X and C-H Borylation of Aryl Halides. *Angew. Chem., Int. Ed.* **2015**, *54*, 11843−11847.

(12) Mfuh, A. M.; Nguyen, V. T.; Chhetri, B.; Burch, J. E.; Doyle, J. D.; Nesterov, V. N.; Arman, H. D.; Larionov, O. V. Additive- and Metal-Free, Predictably 1,2-and 1,3-Regioselective, Photoinduced Dual C-H/C-X Borylation of Haloarenes. *J. Am. Chem. Soc.* **2016**, *138*, 8408−8411.

(13) Li, H.; Shangguan, X.; Zhang, Z.; Huang, S.; Zhang, Y.; Wang, J. Formal carbon insertion of N-tosylhydrazone into B-B and B-Si bonds: gem-diborylation and gem-silylborylation of sp3 carbon. *Org. Lett.* **2014**, *16*, 448−451.

(14) Eichhorn, A. F.; Kuehn, L.; Marder, T. B.; Radius, U. Facile insertion of a cyclic alkyl(amino) carbene carbon into the B-B bond of diboron(4) reagents. *Chem. Commun.* **2017**, *53*, 11694−11696.

(15) Hu, J.; Zhao, Y.; Shi, Z. Highly tunable multi-borylation of gem-difluoroalkenes via copper catalysis. *Nat. Catal.* **2018**, *1*, 860−869.

(16) Teo, W. J.; Yang, X. X.; Poon, Y. Y.; Ge, S. Z. Cobalt-catalyzed deoxygenative triborylation of allylic ethers to access 1,1,3-triborylalkanes. *Nat. Commun.* **2020**, *11*, 5193.

(17) Li, J.; Ge, S. Copper-Catalyzed Quadruple Borylation of Terminal Alkynes to Access sp(3)-Tetra-Organometallic Reagents. *Angew. Chem., Int. Ed. Engl.* **2022**, *61*, No. e202213057.

(18) Darby, N.; Kim, C. U.; Salaün, J. A.; Shelton, K. W.; Takada, S.; Masamune, S. Concerning the 1,5-didehydro[10]annulene system. *J. Chem. Soc. D* **1971**, *0*, 1516−1517.

(19) Jones, R. R.; Bergman, R. G.; p-Benzyne. Generation as an intermediate in a thermal isomerization reaction and trapping evidence for the 1,4-benzenediyl structure. *J. Am. Chem. Soc.* **1972**, *94*, 660−661.

(20) Rule, J. D.; Wilson, S. R.; Moore, J. S. Radical polymerization initiated by Bergman cyclization. *J. Am. Chem. Soc.* **2003**, *125*, 12992−12993.

(21) Perrin, C. L.; Rodgers, B. L.; O'Connor, J. M. Nucleophilic addition to a p-benzyne derived from an enediyne: a new mechanism for halide incorporation into biomolecules. *J. Am. Chem. Soc.* **2007**, *129*, 4795−4799.

(22) Perrin, C. L.; Reyes-Rodriguez, G. J. Reactivity of nucleophiles toward a p-benzyne derived from an enediyne. *J. Phys. Org. Chem.* **2013**, *26*, 206−210.

(23) Wenthold, P. G.; Winter, A. H. Nucleophilic Addition to Singlet Diradicals: Homosymmetric Diradicals. *J. Org. Chem.* **2018**, *83*, 12390−12396.

(24) Maeda, S.; Morokuma, K. Communications: A systematic method for locating transition structures of A plus B -> X type reactions. *J. Chem. Phys.* **2010**, *132*, 24110.

(25) Maeda, S.; Harabuchi, Y. Exploring paths of chemical transformations in molecular and periodic systems: An approach utilizing force. *WIREs Comput. Mol. Sci.* **2021**, *11*, No. e1538.

(26) Sumiya, Y.; Harabuchi, Y.; Nagata, Y.; Maeda, S. Quantum Chemical Calculations to Trace Back Reaction Paths for the Prediction of Reactants. *JACS Au* **2022**, *2*, 1181.

(27) Mita, T.; Harabuchi, Y.; Maeda, S. Discovery of a synthesis method for a difluoroglycine derivative based on a path generated by quantum chemical calculations. *Chem. Sci.* **2020**, *11*, 7569−7577.

(28) Kanna, W.; Harabuchi, Y.; Takano, H.; Hayashi, H.; Maeda, S.; Mita, T. Carboxylation of a Palladacycle Formed via C(sp³)-H Activation: Theory-Driven Reaction Design. *Chem-Asian J.* **2021**, *16*, 4072−4080.

(29) Hayashi, H.; Katsuyama, H.; Takano, H.; Harabuchi, Y.; Maeda, S.; Mita, T. *In silico* reaction screening with difluorocarbene for *N*-difluoroalkylative dearomatization of pyridines. *Nat. Synth.* **2022**, *1*, 804−814.

(30) Takano, H.; Katsuyama, H.; Hayashi, H.; Kanna, W.; Harabuchi, Y.; Maeda, S.; Mita, T. A theory-driven synthesis of symmetric and unsymmetric 1,2-bis(diphenylphosphino)ethane analogues via radical difunctionalization of ethylene. *Nat. Commun.* **2022**, *13*, 7034.

(31) Maeda, S.; Ohno, K.; Morokuma, K. Systematic exploration of the mechanism of chemical reactions: the global reaction route mapping (GRRM) strategy using the ADDF and AFIR methods. *Phys. Chem. Chem. Phys.* **2013**, *15*, 3683−3701.

(32) Maeda, S.; Harabuchi, Y.; Takagi, M.; Saita, K.; Suzuki, K.; Ichino, T.; Sumiya, Y.; Sugiyama, K.; Ono, Y. Implementation and performance of the artificial force induced reaction method in the GRRM17 program. *J. Comput. Chem.* **2018**, *39*, 233−250.

(33) Maeda, S.; Harabuchi, Y. On Benchmarking of Automated Methods for Performing Exhaustive Reaction Path Search. *J. Chem. Theory Comput.* **2019**, *15*, 2111−2115.

(34) Sumiya, Y.; Maeda, S. Rate Constant Matrix Contraction Method for Systematic Analysis of Reaction Path Networks. *Chem. Lett.* **2020**, *49*, 553−564.

(35) Maeda, S.; Harabuchi, Y.; Hayashi, H.; Mita, T. Toward Ab Initio Reaction Discovery Using the Artificial Force Induced Reaction Method. *Annu. Rev. Phys. Chem.* **2023**, *74*, 287−311.

(36) Nicolaou, K. C.; Zuccarello, G.; Riemer, C.; Estevez, V. A.; Dai, W. M. Design, Synthesis, and Study of Simple Monocyclic Conjugated Enediynes - the 10-Membered Ring Enediyne Moiety of the Enediyne Anticancer Antibiotics. *J. Am. Chem. Soc.* **1992**, *114*, 7360−7371.

(37) Nicolaou, K. C.; Zuccarello, G.; Ogawa, Y.; Schweiger, E. J.; Kumazawa, T. Cyclic Conjugated Enediynes Related to Calicheamicins and Esperamicins - Calculations, Synthesis, and Properties. *J. Am. Chem. Soc.* **1988**, *110*, 4866−4868.

(38) Schreiner, P. R. Cyclic enediynes: relationship between ring size, alkyne carbon distance, and cyclization barrier. *Chem. Commun.* **1998**, 483−484.

(39) Mohamed, R. K.; Peterson, P. W.; Alabugin, I. V. Concerted Reactions That Produce Diradicals and Zwitterions: Electronic, Steric, Conformational, and Kinetic Control of Cycloaromatization Processes. *Chem. Rev.* **2013**, *113*, 7089−7129.

(40) Campbell, A.; Peterson, P. W.; Alabugin, I. V. In Aromaticity; Fernandez, I., Ed.; Elsevier, 2021.

(41) Perrin, C. L.; Rodgers, B. L.; O'Connor, J. M. Nucleophilic addition to a p-benzyne derived from an enediyne:: A new mechanism for halide incorporation into biomolecules. *J. Am. Chem. Soc.* **2007**, *129*, 4795−4799.

(42) Hashmi, A. S. K.; Braun, I.; Rudolph, M.; Rominger, F. The Role of Gold Acetylides as a Selectivity Trigger and the Importance of *gem*-Diaurated Species in the Gold-Catalyzed Hydroarylating-Aromatization of Arene-Diynes. *Organometallics* **2012**, *31*, 644−661.

(43) Frisch, M. J.; Trucks, G. W.; Schlegel, H. B.; Scuseria, G. E.; Robb, M. A.; Cheeseman, J. R.; Scalmani, G.; Barone, V.; Petersson, G. A.; Nakatsuji, H.; Li, X.; Caricato, M.; Marenich, A. V.; Bloino, J.; Janesko, B. G.; Gomperts, R.; Mennucci, B.; Hratchian, H. P.; Ortiz, J. V.; Izmaylov, A. F.; Sonnenberg, J. L.; Williams; Ding, F.; Lipparini, F.; Egidi, F.; Goings, J.; Peng, B.; Petrone, A.; Henderson, T.; Ranasinghe, D.; Zakrzewski, V. G.; Gao, J.; Rega, N.; Zheng, G.; Liang, W.; Hada, M.; Ehara, M.; Toyota, K.; Fukuda, R.; Hasegawa, J.; Ishida, M.; Nakajima, T.; Honda, Y.; Kitao, O.; Nakai, H.; Vreven, T.; Throssell, K.; Montgomery, Jr., J. A.; Peralta, J. E.; Ogliaro, F.; Bearpark, M. J.; Heyd, J. J.; Brothers, E. N.; Kudin, K. N.; Staroverov, V. N.; Keith, T. A.; Kobayashi, R.; Normand, J.; Raghavachari, K.; Rendell, A. P.; Burant, J. C.; Iyengar, S. S.; Tomasi, J.; Cossi, M.; Millam, J. M.; Klene, M.; Adamo, C.; Cammi, R.; Ochterski, J. W.; Martin, R. L.; Morokuma, K.; Farkas, O.; Foresman, J. B.; Fox, D. J. *Gaussian 16 Rev. C.01*; Wallingford, CT, 2016.

(44) Choi, C.; Elber, R. Reaction-Path Study of Helix Formation in Tetrapeptides - Effect of Side-Chains. *J. Chem. Phys.* **1991**, *94*, 751−760.